CRYSTAL GROWTH & DESIGN

Article

pubs.acs.org/crystal

Linear Deracemization Kinetics during Viedma Ripening: Autocatalysis Overruled by Chiral Additives

René R. E. Steendam,[†] Janneke Dickhout,[†] Willem J. P. van Enckevort,*[,†] Hugo Meekes,[†] Jan Raap,[‡] Floris P. J. T. Rutjes,[†] and Elias Vlieg[†]

[†]Radboud University Nijmegen, Institute for Molecules and Materials, Heyendaalseweg 135, 6525 ED Nijmegen, The Netherlands

[‡]Leiden Institute of Chemistry, Leiden University, Einsteinweg 55, 2333 CC, Leiden, The Netherlands

ABSTRACT: Viedma ripening proceeds through an autocatalytic feedback mechanism which exponentially deracemizes an initially racemic solid state to an enantiopure end state. Here we show that, in the presence of enantiopure additives with a concentration of as low as 2.5×10^{-2} mol %, Viedma ripening proceeds with an overall linear and faster increase in enantiomeric excess. These experimental results can be explained using a simple model which assumes a difference in growth and dissolution rates between the enantiomers. This model also accounts for the generally observed linearity during the initial stages of Viedma ripening without additives.

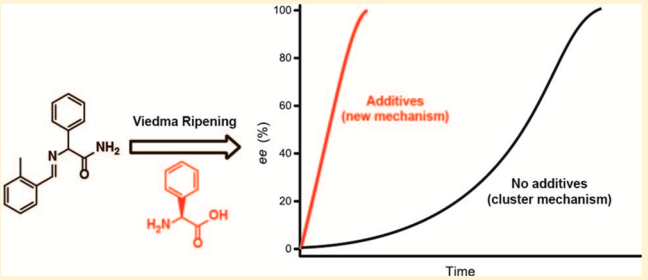

INTRODUCTION

Acquiring enantiopure molecules is of profound importance in many fields of chemistry.[1] Viedma ripening[2,3] is among the most facile and reliable methods available to reach single chirality.[4] It enables the complete solid-state deracemization of molecules that form racemic conglomerate crystals and racemize in solution. To date, many compounds have been deracemized successfully through Viedma ripening.[5,6] The initial symmetry breaking of the solid state, and with that the final configuration of the product, depends on the initial enantiomeric excess (*ee*),[7] the difference in crystal size distribution (CSD) between the enantiomers,[8] unintended chiral impurities,[9] or chiral additives.[7] Chiral additives hamper the crystallization and dissolution of their corresponding enantiomer leading to a difference in CSD between the enantiomers.[10]

In the Viedma ripening process, symmetry breaking is followed by asymmetric amplification of the solid state *ee*, which proceeds through a mechanism that can be explained by taking four processes into account: (1) racemization in solution, (2) Ostwald ripening, (3) attrition, and (4) enantioselective reincorporation of chiral clusters.[11] The effect of enantioselective incorporation of chiral clusters into larger crystallites of the same hand is required to explain the exponential increase in *ee*.[11−15] Enantioselective agglomeration of crystals has been observed experimentally for sodium chlorate and sodium bromate.[16] However, chiral recognition at a smaller scale between clusters and crystals has not been demonstrated yet, although achiral clusters and their interactions have been studied.[17] Nevertheless, apart from a single report,[18] all computational studies in literature based on rate equations,[12,13] Monte Carlo simulations,[14,19] a population balance model,[20] and dispersive kinetic models[21] require a feedback mechanism in terms of clusters to account for the exponential deracemization rate observed in many Viedma ripening experiments.[18,22−25]

Recently, deracemization of conglomerate crystals was accomplished through repeated temperature-induced dissolution and growth of a racemic mixture of crystals in solution.[26] Differences in growth rates of crystals was proposed as the driving force behind this deracemization method using temperature cycling.[27] These growth rate differences can be explained by the nucleation process of the crystals prior to deracemization in which nucleation of both enantiomers occurs at slightly different times and thus at different supersaturation levels. These differences lead to crystals that individually have slightly different defects and therefore slightly different thermodynamic and kinetic properties. Two models have been proposed in which either the mean crystal growth rate or the growth rate dispersion was varied. Starting without a difference in CSD and *ee*, each model resulted in a sigmoidal increase in *ee*. As crystal breakage and agglomeration are not considered and temperature is constant, these models[27] at present cannot be used to explain Viedma ripening.

Here we show experimentally that deracemization through Viedma ripening in the presence of chiral additives leads to a linear instead of the previously observed exponential increase in *ee*. These results can be explained by means of a model which assumes a difference in growth and dissolution rate between the enantiomers.

EXPERIMENTAL SECTION

The herein reported experimental procedures are based on a literature method.[9] Each experiment was conducted using new glassware in

Received: January 28, 2015
Revised: March 2, 2015

DOI: 10.1021/acs.cgd.5b00127
Cryst. Growth Des. XXXX, XXX, XXX−XXX

order to avoid any effect of (chiral) contamination. In these experiments, *N*-(2-methylbenzylidine) phenylglycin amide (**1**) was used from the same batch as the experiments reported previously.[7,9] The *ee* of the starting material (**1**) was found to be 0% within the detection limit (~0.5%) of the chiral HPLC. Polytetrafluoroethylene (PTFE)-coated oval shaped magnetic stirring bars (length 20 mm, ø 10 mm) and scintillation flasks were purchased from VWR. Glass beads (ø = 1.5−2.5 mm), 1,8-diazabicyclo[5.4.0]undec-7-ene (DBU), both enantiomers of phenylglycine (**2**) and acetonitrile (ACN) were purchased from Sigma-Aldrich and used as received. The experiments were conducted at a temperature of 20 ± 2 °C.

Viedma Ripening with Additives. A 20 mL scintillation flask was filled with 400 mg of (*rac*)-**1**, 0.025−200 mg of (*S*)-**2** or (*R*)-**2**, 8 g of glass beads, an oval shaped magnetic stirring bar, and 3.5 g of ACN. For experiments in which a small amount of additive (<1 mg) was used, a stock solution was prepared by dissolving 1 mg of (*S*)-**2** in 4.0 g of ACN from which the required amount of additive was taken. The resulting suspension was ground at 600 rpm for 1 h after which 0.147 mL of DBU was added to start the deracemization process.

Sampling. About 0.2 mL of slurry was withdrawn from the experiment using a pasteur pipet. The sample was immediately subjected to vacuum filtration on a P4 glass filter (ø 10 mm). The residual crystals were washed on the filter using 0.5 mL of methanol in order to remove DBU and mother liquor. The crystals were subsequently dissolved in 1.5 mL of 2-propanol and the *ee* was determined using chiral HPLC.

Determination of *ee* Using Chiral HPLC. A Chiralpak AD-H (250 × 4.6 mm ID) column was used in combination with the following conditions; eluent *n*-heptane/2-propanol (95/5 v/v%), flow 1 mL/min, room temperature, λ = 254 nm, inj. vol. 20 μL. Retention times: (*R*)-**1** 30.1 min, (*S*)-**1** 34.5 min.

Determination of Racemization in Solution. Ten milligrams of (*R*)-**1** was dissolved in 10.0 mL of either ACN or MeOH. To this was added 0.1 mL of a solution containing the catalyst which was prepared by adding 50 μL of DBU (16.9 mol %) in 5.0 mL of either MeOH or ACN. From the resulting solution, 1.0 mL was transferred to an HPLC vial, and the *ee* of the stagnant solution was monitored through time using chiral HPLC analysis. The results are plotted in Figure 11 of Appendix B.

EXPERIMENTAL RESULTS

To study the effect of additives on Viedma ripening, experiments were conducted using a model system involving an amino acid derivative (Figure 1, compound **1**).[7] The enantiopure additive

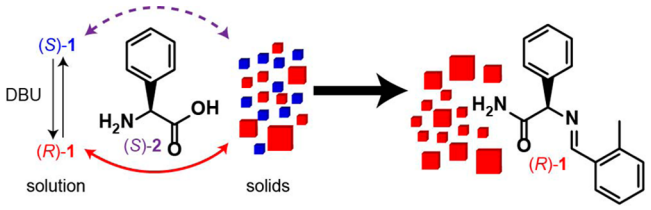

Figure 1. Schematic representation of the deracemization of compound **1** through Viedma ripening. Chiral additive (*S*)-**2** enantiomerically hampers the crystal growth of (*S*)-**1** leading to different growth and dissolution rates for (*S*)-**1** and (*R*)-**1**, and ultimately an enantiopure (*R*)-**1** end state is obtained.

(*S*)- or (*R*)-phenylglycine (**2**) is able to enantioselectively affect the crystallization of its corresponding enantiomer of compound **1**. This leads to different crystallization and dissolution rates between the enantiomers. As a result, deracemization proceeds to give enantiopure **1** of which the final handedness of **1** is opposite to the handedness of the additive **2** (known as Lahav's rule of reversal).[28]

The evolution of *ee* during Viedma ripening in the absence and presence of chiral additives is shown in Figure 2a. Without additives, the initial racemic solid state slowly becomes enantiomerically enriched after which the *ee* increases exponentially. Adding a small amount (0.4 mol %) of additive results in a much faster deracemization rate in which the *ee* was found to increase in a linear fashion.

The linear increase was reproducibly found for different amounts of additive for experiments conducted in acetonitrile (ACN, Appendix A1). In a previous report, the additive amount used varied from 0.1 to 8.7 mol %.[7] The fastest deracemization rate in our experiments was found to be in the presence of about 1 mol % of additive (Figure 2b). Similar linear growth kinetics was observed during Viedma ripening experiments conducted in methanol (MeOH, Appendix A2). In this case the deracemization rate was lower, which can be explained by slower racemization of **1** in MeOH (Appendix B). For additive concentrations above 80 mol % deracemization of **1** is almost completely inhibited.

MODELING RESULTS

Model Description. To understand the linear behavior of the observed $ee(t)$ curves, we start with the simple model for Viedma ripening as described previously,[11] which is based on the original model of Uwaha.[12−15] The only difference with the previous model is that we now allow for a difference in growth and dissolution rates between the enantiomers. This is based upon the experimental observation of a different size distribution between the enantiomers in the presence of enantiopure additives during grinding.[10] In this model only two crystal sizes are taken into account: big crystals (containing in total B^+ and B^- molecules of the two enantiomers) and clusters (containing C^+ and C^- molecules altogether). Figure 3 schematizes the various processes involved in the deracemization procedure, which is described by the set of coupled differential eqs 1a−1d with analogous equations for the opposite enantiomer.

$$\frac{\partial B^+}{\partial t} = a^+B^+(M^+ - M_{eq}^B) - bB^+ + cC^+B^+ \quad (1a)$$

$$\frac{\partial C^+}{\partial t} = bB^+ + a^+C^+(M^+ - M_{eq}^C) - cC^+B^+ \quad (1b)$$

$$\frac{\partial M^+}{\partial t} = -a^+B^+(M^+ - M_{eq}^B) - a^+C^+(M^+ - M_{eq}^C) - d(M^+ - M^-) \quad (1c)$$

$$T = B^+ + C^+ + B^- + C^- + M^+ + M^- = \text{constant} \quad (1d)$$

The solid phase *ee* is defined as

$$ee = \frac{(B^+ + C^+) - (B^- + C^-)}{(B^+ + C^+) + (B^- + C^-)} \quad (2)$$

We assume an ablation rate (formation of small chiral clusters by grinding) proportional to the number of large crystals of each enantiomer, bB. As fractured crystals are studded with growth steps and the advancement of steps is proportional to supersaturation, we consider linear growth kinetics. This means that the growth and dissolution rate of large crystals and small clusters is proportional to the difference in actual solute concentration and the equilibrium concentration of the solution in contact with the large crystals and small clusters, $a^{\pm}(M^{\pm} - M_{eq}^{B/C})$. As a consequence of the Gibbs−Thomson effect, the equilibrium concentration of the solution in contact with the

DOI: 10.1021/acs.cgd.5b00127
Cryst. Growth Des. XXXX, XXX, XXX−XXX

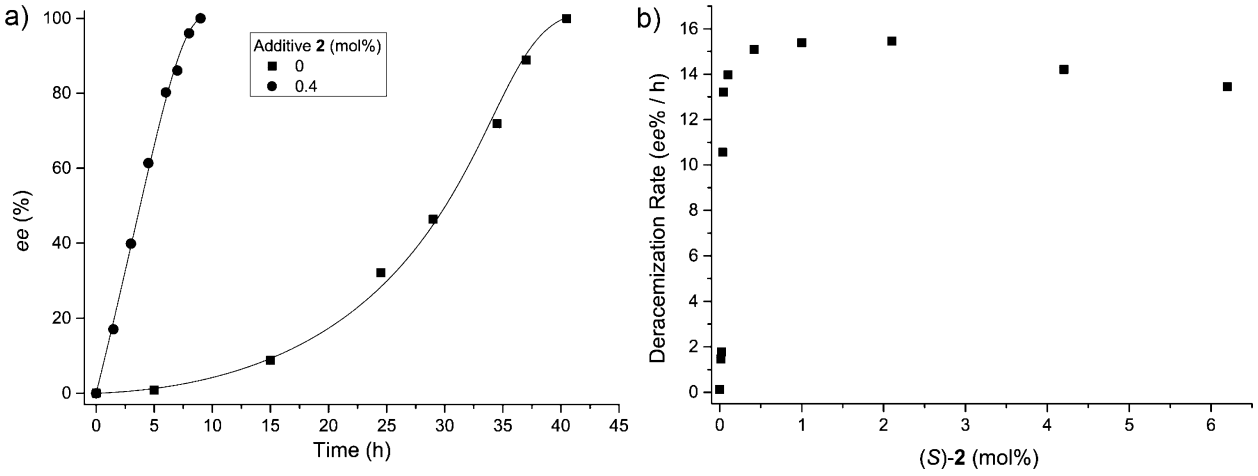

Figure 2. Viedma ripening experiments conducted in ACN. (a) In the absence of additives, the *ee* of **1** is amplified in a sigmoidal fashion, whereas a linear increase in *ee* is observed when chiral additive **2** was used. The lines are a guide to the eye. (b) Initial rate, d*ee*/d*t*, of deracemization as a function of the amount of additive.

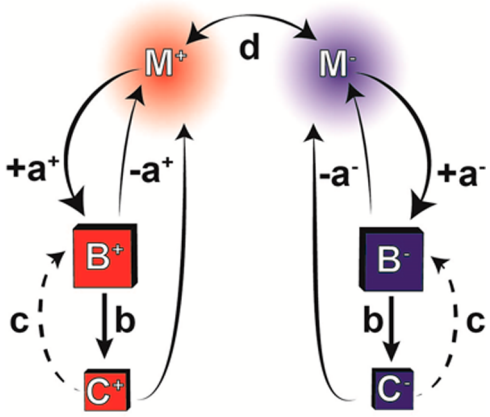

Figure 3. Schematic view of the processes involved during Viedma ripening.

small clusters, M^C_{eq}, is larger than that of the large crystals M^B_{eq}. The incorporation rate of small clusters into the large crystals of the same handedness is second order, proportional to both the number of large crystals and the number of small clusters, i.e., *cCB*. We assume no incorporation of small clusters into large crystals of opposite handedness. Finally, the racemization rate constant in solution is defined by *d*, where we assume that the racemization rate is proportional to the difference in concentration of both enantiomers, $d(M^+ - M^-)$. All the parameters used are listed in Table 1.

To follow the process of deracemization in time, the set of eqs 1a−1d is numerically integrated using the finite difference method. Similar to the experiments, the system was "premixed" for some period prior to the $ee(t)$ runs, keeping $a^+ = a^- = (a^+ + a^-)/2$, not allowing racemization in the liquid and starting from $B^+ = B^-$ and $C^+ = C^- = 0$. This gives $ee(t = 0) = 0$, an equal size distribution of both enantiomers (i.e., $B^+ = B^- = B_0$ and $C^+ = C^- = C_0$) and avoids initial fluctuations in $ee(t)$. In all simulation runs we kept $M^B_{eq} = 1.0$ and $M^C_{eq} = 1.1$.

Simulations. In earlier work, Viedma ripening in the absence of chiral additives was explained by the reincorporation of tiny chiral clusters ($c \neq 0$) produced by grinding, into the larger crystals of the same handedness.[11] This leads to sigmoid shaped $ee(t)$ curves as was also observed in many experiments.[22−25] In our model (i.e., eqs 1a−1d) this situation corresponds to $a^+ = a^-$ and $c \neq 0$ (Figure 4, solid line). Chiral additives or chiral impurities reduce the growth and dissolution rate of chiral crystals of the same handedness.[7,9,10] Therefore, adding chiral additives to the system leads to slightly different values of the kinetic coefficients a^+ and a^-. Simulations using a fixed $c \neq 0$ show that upon introducing a difference between a^+ and a^- leads to a change in curve shape which becomes more and more linear as shown in Figure 4. The additive effect almost completely overrules the cluster effect provided that the additive effect is sufficiently large ($a^+ - a^- = 0.50$, Figure 4). In addition, deracemization proceeds much faster when enantiopure additives are present.

No Clusters Required for Complete Deracemization. We find that there is no need for cluster incorporation to achieve full deracemization by grinding, provided that $a^+ \neq a^-$. Solving the set of coupled differential equations with $c = 0$ and $\partial\#/\partial t = 0$ gives four steady state solutions at $t = \infty$. This follows

Table 1. Variables and Constants Used in This Study[a]

B^+, B^-	Number of molecules in large crystals of the + and − enantiomer
C^+, C^-	Number of molecules in small crystal clusters of the + and − enantiomer
M	Total number of monomer molecules in solution
M^+, M^-	Number of monomer molecules of the + and − molecules in solution
t	Time
M^B_{eq}	Equilibrium number of molecules in solution in contact with the big crystals of each enantiomer
M^C_{eq}	Equilibrium number of molecules in solution when in contact with the small clusters of each enantiomer
T	Total number of molecules in the solid phase and solution
ee	Enantiomeric excess in the solid phase
a^+, a^-	Kinetic coefficients for growth and dissolution of the + and − enantiomer
b	Rate constant for ablation of big crystals
c, c^+, c^-	Rate constants for the incorporation of chiral clusters into big crystals
d	Rate constant for racemization in solution
k	Rate constant for deracemization at start; $[\partial ee(t)/\partial t]_{t\approx 0} = k$

[a]All numbers and rates have relative meaning only.

DOI: 10.1021/acs.cgd.5b00127
Cryst. Growth Des. XXXX, XXX, XXX−XXX

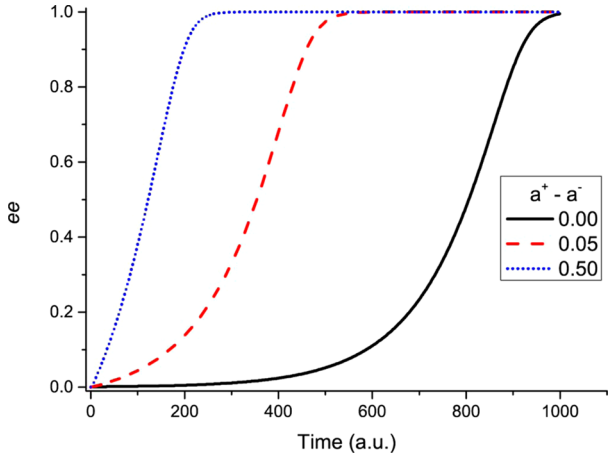

Figure 4. Simulations of Viedma ripening experiments as a function of the amount of additive, corresponding to a specific difference in $(a^+ - a^-)$ for fixed c. Simulation parameters: $ee(t = 0) = 0.001$; $c = 0.01$; $a^- = 5.00$; $d = 10$.

from solving eqs 3a−3c, eq 1d and the analogous equations for the opposite enantiomer.

$$a^+B^+(M^+ - M^B_{eq}) - bB^+ = 0 \quad (3a)$$

$$a^+C^+(M^+ - M^C_{eq}) + bB^+ = 0 \quad (3b)$$

$$-a^+B^+(M^+ - M^B_{eq}) - a^+C^+(M^+ - M^C_{eq}) - d(M^+ - M^-) = 0 \quad (3c)$$

The four solutions are

(i) $B^- = 0$, $C^- = 0$, with $B^+ + C^+ = T - M$ and $ee = 1$
(ii) $B^+ = 0$, $C^+ = 0$, with $B^- + C^- = T - M$ and $ee = -1$
(iii) B^- and $B^+ \neq 0$, this solution is only possible if $a^+ = a^-$
(iv) $B^- = B^+ = C^- = C^+ = 0$, if all crystals are dissolved in M by too intense grinding (i.e., b is too large).

In all four cases the solution gives $M^+ = M^- = 0.5M$, regardless of $d > 0$. Only solutions (i) and (ii) are relevant and show that at $t = \infty$, enantiopure material is obtained by Viedma ripening without the need for cluster incorporation (i.e., it is possible to have $c = 0$) into the big crystals in the case $a^+ \neq a^-$.

Deracemization Kinetics. The set of differential eqs 1a−1d cannot be solved exactly, but needs approximations to derive an analytical expression for the deracemization rate constant, $k = ee(t)/t$ (see Appendix C). For $c = 0$ and fast racemization, i.e., $d \to \infty$, this gives

$$k \approx b(a^+ - a^-)/(a^+ + a^-) \quad (4)$$

This demonstrates that the kinetics are indeed linear. Equation 4 further shows that in this approximation k practically only depends on the grinding rate b and the kinetic coefficients a^+ and a^-, and is almost independent of the total amount of chiral molecules, and the equilibrium concentrations. Figure 5a shows a simulated $ee(t)$ curve (dashed line) for $c = 0$, $ee(t = 0) = 0$ and $d = \infty$ and the comparison with the linear relation $ee(t) = kt$ (solid line), with k given by eq 4. For low values of t an excellent fit is obtained. To validate this expression for different parameters, a successful comparison has been made between k values obtained from simulations and calculated k using eq 4 (Figure 5b).

Additive Versus Cluster Effect. Both the additive and the cluster effect can act simultaneously ($c \neq 0$ and $a^+ \neq a^-$). Numerous simulations using a variety of parameters and instantaneous racemization in solution indeed show in every case that eq 4 is approximately satisfied. Figure 6a displays k versus $b((a^+ - a^-)/(a^+ + a^-))$ curves for three values of c and shows that the linear curves coincide for all c. In other words, k is independent of c and the difference between a^+ and a^- gives the $ee(t)$ curve an initial "boost" with slope k. For further time t, the $ee(t)$ curve turns sigmoidal and the cluster effect determines the deracemization process as shown in Figure 6b.

Chiral additives or impurities may also affect the incorporation of the clusters into the larger crystals, resulting in different clustering rates (i.e., $c^+ \neq c^-$). Figure 7a shows an $ee(t)$ curve for $c^+ \neq c^-$, $ee(t = 0) = 0$ and $a^+ = a^-$. Again $k \neq 0$, but also sigmoidal characteristics can be observed. In this case the initial deracemization rate is found to depend almost linearly on $c^+ - c^-$ (Figure 7b). A complete expression for k is beyond the scope of our study. A combination of $a^+ \neq a^-$ and $c^+ \neq c^-$ gives sigmoidal curves and again with $k \neq 0$.

Effect of Racemization Rate. To verify the effect of slower racemization rates in solution, simulation runs have been performed for a range of d values. For all values of d the simulation runs with $a^+ \neq a^-$ and $c = 0$ again produce linear $ee(t)$ curves except for large t as shown in Figure 8. Thus, the initial linearity persists independently of racemization rate. This corresponds to our linear $ee(t)$ curves of Viedma ripening experiments conducted in both ACN (fast racemization) and MeOH (slow racemization). The deracemization rate constant, k,

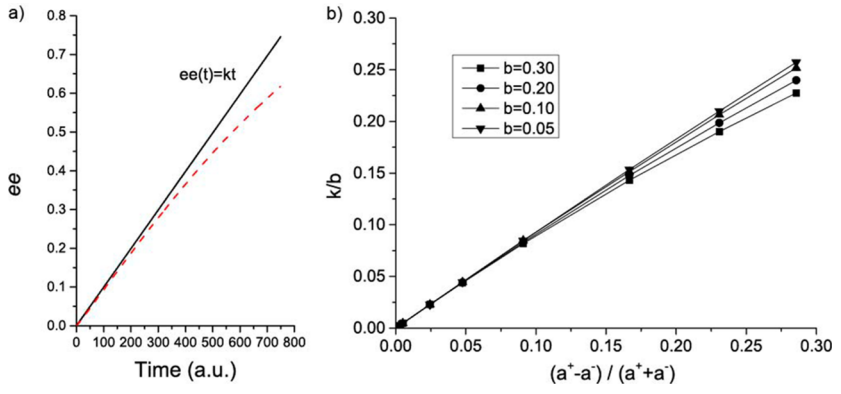

Figure 5. (a) Simulated $ee(t)$ (dashed line) and a fit with $ee(t) = kt$ (solid line) with $a^+ = 5.05$; $a^- = 5.00$; $b = 0.2$; $c = 0$. (b) k/b obtained from simulated $ee(t)$ slopes at $t = 0$ as a function of $(a^+ - a^-)/(a^+ + a^-)$ for different values of a^+ and b, keeping $a^- = 10.0$, $c = 0$ and $d = \infty$. If eq 4 is perfectly satisfied, the slope of the curve is 1.0, which holds well for the smaller values of $(a^+ - a^-)/(a^+ + a^-)$ and b.

DOI: 10.1021/acs.cgd.5b00127
Cryst. Growth Des. XXXX, XXX, XXX−XXX

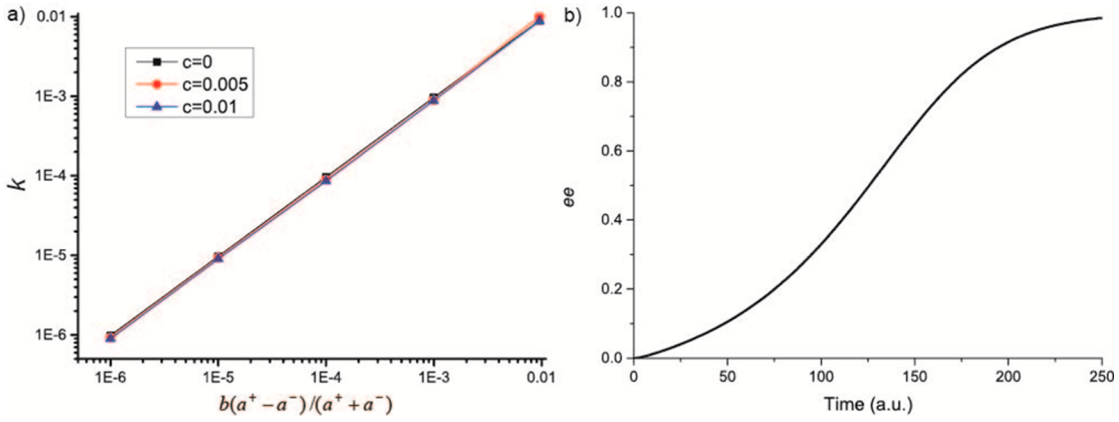

Figure 6. (a) k versus $b((a^+ - a^-)/(a^+ + a^-))$ for three values of c, showing that the initial slope of the $ee(t)$ curve is solely determined by a^+, a^- ,and b, and not by c. (b) After an initial linear increase ($(a^+ - a^-) = 0.10$), the cluster effect ($c = 0.008$) takes over, resulting in a sigmoidal increase in ee for larger $ee(t)$. Simulation parameters: $ee(t = 0) = 0.0$; $a^- = 5.00$; $b = 0.2$; $d = 500$; $M^C_{eq} = 1.1$; $M^B_{eq} = 1.0$.

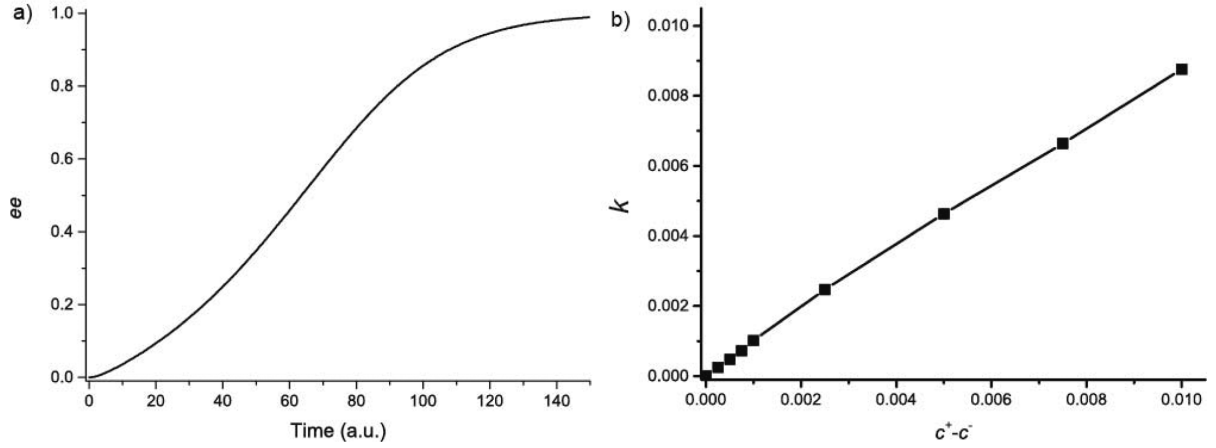

Figure 7. Different cluster incorporation rates $c^+ \neq c^-$ and $a^+ = a^-$: (a) $ee(t)$ curve showing that $k \neq 0$; (b) Linear dependence of k on $(c^+ - c^-)$. In (a) ($a = 5.0$; $c^+ = 0.015$; $c^- = 0.01$); in (b) ($a = 5.0$; $b = 0.2$; $c^- = 0.01$).

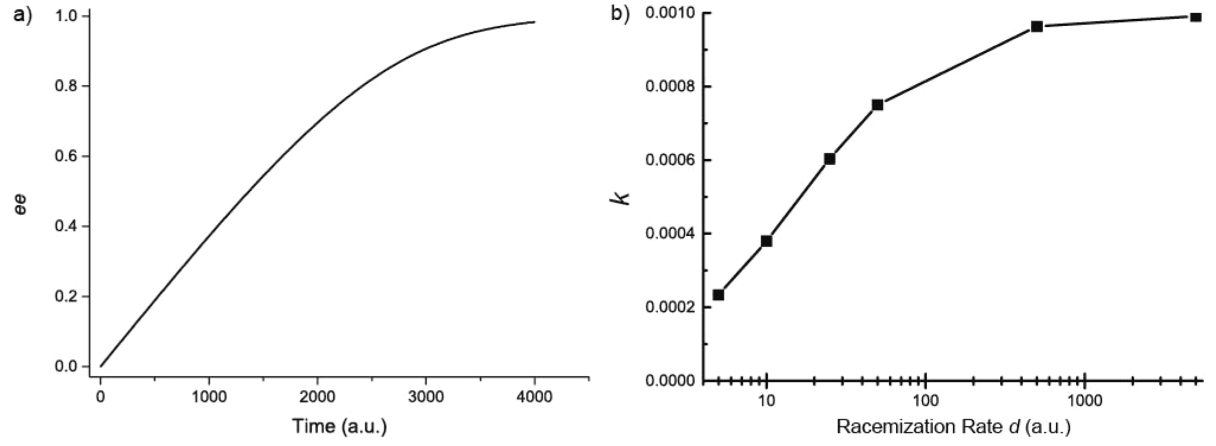

Figure 8. Effect of slower racemization in the solution: (a) regardless of the racemization rate, the onset of the $ee(t)$ curve is always linear; (b) k as a function of racemization rate d in the solution. Simulation parameters: $a^+ = 5.05$; $a^- = 5.00$; $b = 0.2$; $c = 0$. In (a), $d = 10$.

decreases for decreasing d, as expected (Figure 8b). But the linearity of $ee(t)$ for initial t persists.

DISCUSSION OF EXPERIMENTS AND SIMULATIONS

Both our experiments and our model show linear $ee(t)$ curves. For the experiments the linearity persists almost to $ee(t) = 1$, with a large slope k. This indicates that the enantiopure additive leads to a difference in the growth and dissolution rates between the enantiomers (i.e., the difference between a^+ and a^-), which completely overrules the effect of cluster incorporation.

Both compound **1** and additive **2** were used previously,[7] and in that work the $ee(t)$ curves showed both linear and sigmoidal characteristics similar to Figure 4. The main difference between both series of experiments is the deracemization time.

DOI: 10.1021/acs.cgd.5b00127
Cryst. Growth Des. XXXX, XXX, XXX−XXX

The downscaling in our experiments results in a 1−2 orders of magnitude larger grinding rate (i.e., b in our model) that leads to a 50 times faster deracemization rate as compared to the previous study.[7] This in turn leads to a large k-value, overruling the effect of cluster incorporation, giving almost completely linear $ee(t)$ curves in contrast to the previous report.[7]

For very high additive concentrations k does not increase anymore in our experiments (Appendix A). Possibly the surface of the crystals is completely covered by the additive of the same handedness, so a "saturation" of $(a^+ - a^-)$ occurs. It is also possible that a high chiral additive concentration hinders the growth rate of the opposite enantiomer as well.

Following the simplest model, the initial slope of $ee(t)$ is $k \approx b((a^+ - a^-)/(a^+ + a^-))$. This implies that the effect of chiral additives on Viedma ripening is largest if the additive induces a difference in growth rates between both enantiomers, $(a^+ - a^-)$ and the grinding rate (b) is large. However, one cannot exclude additive adsorption effects on the incorporation rate of clusters. Also the rate of solution racemization plays a role. Both affect the time development of the solid state ee, but in all cases the $ee(t)$ curve is linear for not too large t and its initial slope is larger than zero.

Recently, another model for Viedma ripening has been proposed, which is based on crystal size dependent growth rates by introducing a frequency term in the crystal growth rate expressions.[18] This gives comparable sigmoid $ee(t)$ curves as observed for the cluster model. We expect that also for these approaches a difference in growth rates, $a^+ \neq a^-$, gives the $ee(t)$ curves an initial "boost" with slope k. This will be verified in a forthcoming paper.

CONCLUSIONS

Deracemization through Viedma ripening was experimentally found to proceed in a linear fashion when enantiopure additives are present. This can be explained by taking a difference in growth and dissolution rates between the enantiomers into account. The model gives a linear onset of the solid state $ee(t)$ curve. A competition between the additive effect and the effect of chiral cluster incorporation into the enantiomer of the same handedness will take place if time progresses. If the additive effect is dominant, then the $ee(t)$ curve remains linear for large t and deracemization proceeds fast. If the effect of the additive is less strong, then the cluster incorporation effect (or another sigmoidal $ee(t)$ curve forming phenomenon) will take over and the $ee(t)$ curve becomes sigmoidal for larger t. But also in this case deracemization proceeds faster. In addition, we showed that complete deracemization can be achieved by Viedma ripening without the need of cluster incorporation effects, when chiral additives induce a difference in growth rate between both enantiomers.

APPENDIX A: VIEDMA RIPENING EXPERIMENTS WITH ADDITIVES

In acetonitrile (ACN), the linear increase in ee was reproducibly found for different amounts of additive (Figure 9).

We found that deracemization of compound **1** in methanol (MeOH) instead of ACN again proceeded in a linear fashion when additives were present (Figure 10). The racemization rate of **1** was found to be significantly slower in MeOH, which is probably due to hydrogen bonding interactions with the solvent (Figure 11, Appendix B). The half-life time of racemization in ACN (68 min) was found to be 6 times smaller than in

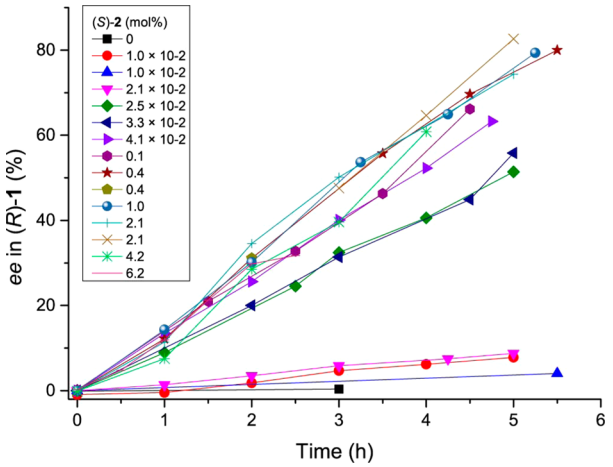

Figure 9. Deracemization experiments conducted in ACN. Linear increase in ee for different amounts of additive. The rate of deracemization as a function of the amount of additive calculated from linear fits of the data is shown in Figure 2b in the main text.

MeOH (420 min). As a result, the deracemization rate in MeOH is much smaller than in ACN, and a larger amount of additive is required to significantly increase the deracemization rate (Figure 10). About 20 mol % of additive was found to maximally increase the ee in Viedma ripening experiments conducted in MeOH. A larger amount of additive leads to a substantial decrease in the deracemization rate.

APPENDIX B: SOLUTION PHASE RACEMIZATION

Figure 11 shows the experimental results of solution phase racemization of compound **1** in both ACN and MeOH.

APPENDIX C: APPROXIMATE EXPRESSION FOR THE DERACEMIZATION RATE CONSTANT

The set of coupled differential eqs 1a−1d in the main text is given below once more, but now with $c = 0$ and instantaneous racemization in solution. This set cannot be solved analytically in an exact manner. To find an expression for the deracemization rate constant k, approximations have to be made.

$$\frac{\partial B^+}{\partial t} = a^+B^+(M - M_{eq}^B) - bB^+ \tag{C1a}$$

$$\frac{\partial C^+}{\partial t} = bB^+ + a^+C^+(M - M_{eq}^C) \tag{C1b}$$

with analogous equations for the opposite enantiomer.

$$\frac{\partial M}{\partial t} = -a^+B^+(M - M_{eq}^B) - a^+C^+(M - M_{eq}^C) - a^-B^-(M - M_{eq}^B) - a^-C^-(M - M_{eq}^C) \tag{C1c}$$

$$T = B^+ + C^+ + B^- + C^- + M \tag{C1d}$$

After premixing as described in the main text, at the start $(t = 0)$ of the deracemization simulation run $B_0^+ = B_0^- = B_0$, $C_0^+ = C_0^- = C_0$ and $ee(t = 0) = 0$. Careful examination of the evolution of B^+, B^-, C^+ and C^- reveals a linear behavior for t not too large for nearly all conditions (Figure 12) according to

$$B^+ = B_0(1 + pt) \tag{C2a}$$

$$B^- = B_0(1 - pt) \tag{C2b}$$

DOI: 10.1021/acs.cgd.5b00127
Cryst. Growth Des. XXXX, XXX, XXX−XXX

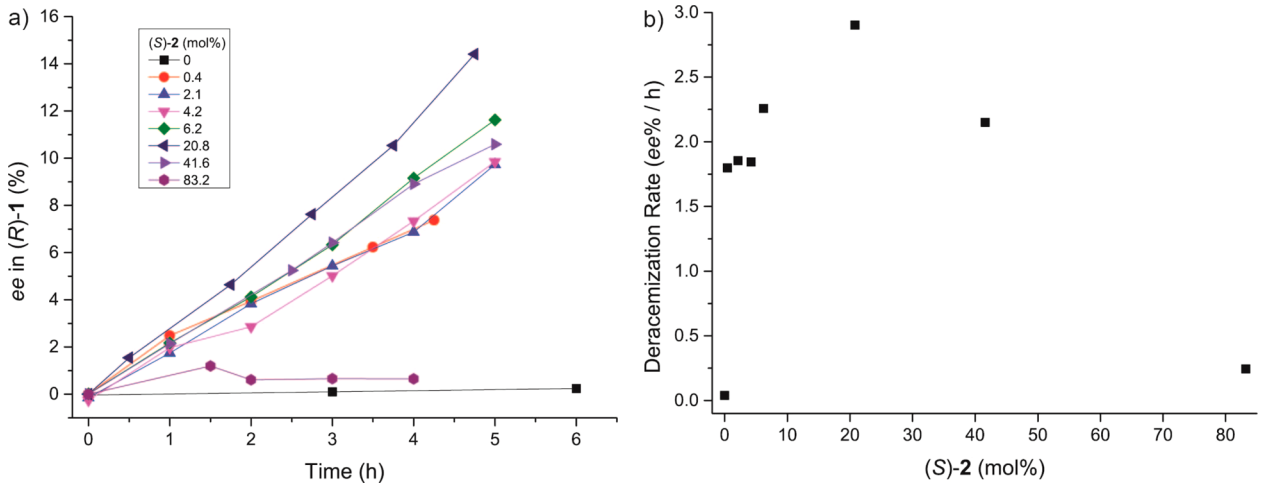

Figure 10. Deracemization experiments conducted in MeOH. (a) Linear increase in *ee* for different amounts of additive. (b) Rate of deracemization as a function of the amount of additive calculated from linear fits of the data in panel a. The scales are different as compared to Figures 2b and 9.

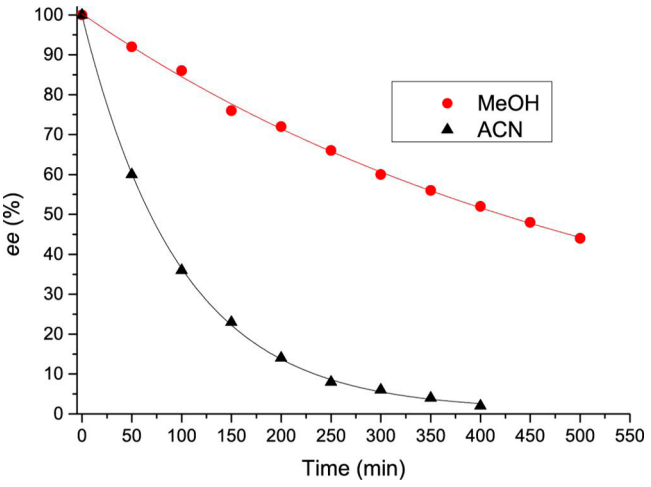

Figure 11. Racemization of compound **1** in a stagnant solution of MeOH ($t_{1/2}$ = 419.79 min) and ACN ($t_{1/2}$ = 68.53 min) in the presence of DBU (16.9 mol %). The data points are fitted with asymptotic functions from which the racemization half-lives were determined.

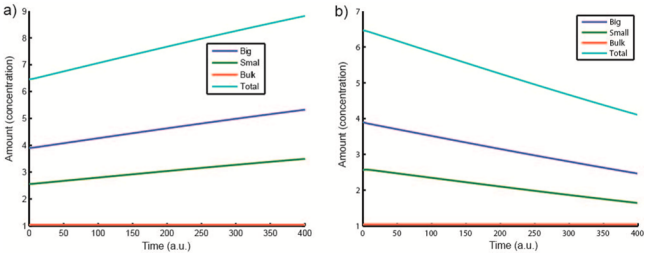

Figure 12. (a) Evolution of B^+, C^+, $B^+ + C^+$, and M as a function of time for the + enantiomer. (b) Evolution of B^-, C^-, $B^- + C^-$, and M as a function of time for the − enantiomer. Here $a^+ > a^-$.

$$C^+ = C_0(1 + pt) \tag{C2c}$$

$$C^- = C_0(1 - pt) \tag{C2d}$$

We use these semiempirical expressions as a starting point in deriving an expression for k.

As $(B^+ + B^- + C^+ + C^-) = 2(B_0 + C_0)$ is constant,

$$\frac{\partial ee(t)}{\partial t} = \frac{1}{2(B_0 + C_0)}\left[\frac{\partial B^+}{\partial t} + \frac{\partial C^+}{\partial t} - \frac{\partial B^-}{\partial t} - \frac{\partial C^-}{\partial t}\right] \tag{C3}$$

or

$$\frac{\partial ee(t)}{\partial t} = \frac{1}{2(B_0 + C_0)}[B_0 + C_0 + B_0 + C_0]p \tag{C4}$$

so

$$\frac{\partial ee(t)}{\partial t} = p = k \tag{C5}$$

So, p is identical to the rate constant k, we searched for.

To obtain an equation for p, we first need an expression for $\Delta M_B = M - M_{B,eq}$. Using the fact that $(\partial B^+/\partial t) = -(\partial B^-/\partial t)$ and eqs C1a−C1b, we get

$$(a^+B^+\Delta M_B - bB^+) = -(a^-B^-\Delta M_B - bB^-) \tag{C6}$$

or

$$\Delta M_B[a^+B_0(1 + pt) + a^-B_0(1 - pt)] = 2bB_0 \tag{C7}$$

or

$$\Delta M_B[(a^+ + a^-) + (a^+ - a^-)pt] = 2b \tag{C8}$$

So, for $pt \ll 1$ and $(a^+ - a^-) \ll (a^+ + a^-)$

$$\Delta M_B[(a^+ + a^-)] \cong 2b \tag{C9}$$

this gives

$$\Delta M_B = \frac{2b}{(a^+ + a^-)} \tag{C10}$$

Now, we are searching for k. Using eq C1a and the fact that $(\partial B^+/\partial t) = pB_0$ we obtain

$$\frac{\partial B^+}{\partial t} = (a^+\Delta M_B - b)B^+ = pB_0 \tag{C11}$$

or

$$(a^+\Delta M_B - b)B_0(pt + 1) = pB_0 \tag{C12}$$

DOI: 10.1021/acs.cgd.5b00127
Cryst. Growth Des. XXXX, XXX, XXX−XXX

As $pt \ll 1$ we now obtain

$$a^{+}\Delta M_B - b = p \tag{C13}$$

and using the relation C10 for ΔM_B this gives

$$p = a^{+}\frac{2b}{(a^{+} + a^{-})} - b \tag{C14}$$

or

$$p = k = b\frac{(a^{+} - a^{-})}{(a^{+} + a^{-})} \tag{C15}$$

AUTHOR INFORMATION

Corresponding Author

*E-mail: w.vanenckevort@science.ru.nl.

Notes

The authors declare no competing financial interest.

ACKNOWLEDGMENTS

Financial support for this work was provided by The Dutch Astrochemistry Network financed by The Netherlands Organisation for Scientific Research (NWO).

REFERENCES

(1) Prelog, V. *Science* **1976**, *193*, 17−24.
(2) Viedma, C. *Phys. Rev. Lett.* **2005**, *94*, 065504−1−065504−4.
(3) Noorduin, W. L.; Meekes, H.; van Enckevort, W. J. P.; Millemaggi, A.; Leeman, M.; Kaptein, B.; Kellogg, R. M.; Vlieg, E. *Angew. Chem., Int. Ed.* **2008**, *47*, 6445−6447.
(4) Lorenz, H.; Seidel-Morgenstern, A. *Angew. Chem., Int. Ed.* **2014**, *53*, 1218−1250.
(5) McLaughlin, D. T.; Nguyen, T. P. T.; Mengnjo, L.; Bian, C.; Leung, Y. H.; Goodfellow, E.; Ramrup, P.; Woo, S.; Cuccia, L. A. *Cryst. Growth Des.* **2014**, *14*, 1067−1076.
(6) Steendam, R. R. E.; Brouwer, M. C. T.; Huijs, E. M. E.; Kulka, M. W.; Meekes, H.; van Enckevort, W. J. P.; Raap, J.; Rutjes, F. P. J. T.; Vlieg, E. *Chem.—Eur. J.* **2014**, *20*, 13527−13530.
(7) Noorduin, W. L.; Izumi, T.; Millemaggi, A.; Leeman, M.; Meekes, H.; Van Enckevort, W. J. P.; Kellogg, R. M.; Kaptein, B.; Vlieg, E.; Blackmond, D. G. *J. Am. Chem. Soc.* **2008**, *130*, 1158−1159.
(8) Kaptein, B.; Noorduin, W. L.; Meekes, H.; van Enckevort, W. J. P.; Kellogg, R. M.; Vlieg, E. *Angew. Chem., Int. Ed.* **2008**, *47*, 7226−7229.
(9) Steendam, R. R. E.; Harmsen, B.; Meekes, H.; van Enckevort, W. J. P.; Kaptein, B.; Kellogg, R. M.; Raap, J.; Rutjes, F. P. J. T.; Vlieg, E. *Cryst. Growth Des.* **2013**, *13*, 4776−4780.
(10) Noorduin, W. L.; van der Asdonk, P.; Meekes, H.; van Enckevort, W. J. P.; Kaptein, B.; Leeman, M.; Kellogg, R. M.; Vlieg, E. *Angew. Chem., Int. Ed.* **2009**, *48*, 3278−3280.
(11) Noorduin, W. L.; van Enckevort, W. J. P.; Meekes, H.; Kaptein, B.; Kellogg, R. M.; Tully, J. C.; McBride, J. M.; Vlieg, E. *Angew. Chem., Int. Ed.* **2010**, *49*, 8435−8438.
(12) Uwaha, M. *J. Phys. Soc. Jpn.* **2004**, *73*, 2601−2603.
(13) Uwaha, M. *J. Phys. Soc. Jpn.* **2008**, *77*, 083802−1−083802−4.
(14) Katsuno, H.; Uwaha, M. *J. Cryst. Growth* **2009**, *311*, 4265−4269.
(15) Uwaha, M.; Katsuno, H. *J. Phys. Soc. Jpn.* **2009**, *78*, 023601−1−023601−4.
(16) Viedma, C.; McBride, J. M.; Kahr, B.; Cintas, P. *Angew. Chem., Int. Ed.* **2013**, *52*, 10545−10548.
(17) Li, D.; Nielsen, M. H.; Lee, J. R. I.; Frandsen, C.; Banfield, J. F.; De Yoreo, J. J. *Science* **2012**, *336*, 1014−1018.
(18) Gherase, D.; Conroy, D.; Matar, O. K.; Blackmond, D. G. *Cryst. Growth Des.:* **2014**, *14*, 928−937.
(19) Saito, Y.; Hyuga, H. *J. Cryst. Growth* **2011**, *318*, 93−98.
(20) Iggland, M.; Mazzotti, M. *Cryst. Growth Des.* **2011**, *11*, 4611−4622.
(21) Skrdla, P. J. *Cryst. Growth Des.* **2011**, *11*, 1957−1965.
(22) Iggland, M.; Fernández-Ronco, M. P.; Senn, R.; Kluge, J.; Mazzotti, M. *Chem. Eng. Sci.* **2014**, *111*, 106−111.
(23) Spix, L.; Alfring, A.; Meekes, H.; van Enckevort, W. J. P.; Vlieg, E. *Cryst. Growth Des.* **2014**, *14*, 1744−1748.
(24) van der Meijden, M. W.; Leeman, M.; Gelens, E.; Noorduin, W. L.; Meekes, H.; van Enckevort, W. J. P.; Kaptein, B.; Vlieg, E.; Kellogg, R. M. *Org. Process Res. Dev.* **2009**, *13*, 1195−1198.
(25) Hein, J. E.; Huynh Cao, B.; Viedma, C.; Kellogg, R. M.; Blackmond, D. G. *J. Am. Chem. Soc.* **2012**, *134*, 12629−12636.
(26) Suwannasang, K.; Flood, A. E.; Rougeot, C.; Coquerel, G. *Cryst. Growth Des.* **2013**, *13*, 3498−3504.
(27) Suwannasang, K.; Coquerel, G.; Rougeot, C.; Flood, A. E. *Chem. Eng. Technol.* **2014**, *37*, 1329−1339.
(28) Addadi, L.; Berkovitchyellin, Z.; Domb, N.; Gati, E.; Lahav, M.; Leiserowitz, L. *Nature* **1982**, *296*, 21−26.

DOI: 10.1021/acs.cgd.5b00127
Cryst. Growth Des. XXXX, XXX, XXX−XXX